The Alignment of Objects with Smooth Surfaces

RONEN BASRI

Department of Brain and Cognitive Science and the A.I. Lab., MIT, Cambridge, MA 02139

AND

SHIMON ULLMAN

*Department of Brain and Cognitive Science and the A.I. Lab., MIT, Cambridge, MA 02139 and Department of Applied Math,
The Weizmann Institute of Science, Rehovot, Israel*

This paper examines the recognition of rigid objects bounded by smooth surfaces, using an alignment approach. The projected image of such an object changes during rotation in a manner that is generally difficult to predict. An approach to this problem is suggested, using the 3D surface curvature at the points along the silhouette. The curvature information requires a single number for each point along the object's silhouette, the radial curvature at the point. We have implemented this method and tested it on images of complex 3D objects. Models of the viewed objects were acquired using three images of each object. The implemented scheme was found to give accurate predictions of the objects' appearances for large transformations. Using this method, a small number of (viewer-centered) models can be used to predict the new appearance of an object from any given viewpoint. © 1993 Academic Press, Inc.

1. INTRODUCTION

Visual object recognition requires the identification of objects observed from different viewpoints. In recent years several attempts have been made to approach this problem using an alignment approach [10, 17, 9, 7, 12, 16, 22, 23]. Many of these attempts have been concentrated on handling either planar or polyhedral objects. In this paper we consider the recognition of rigid objects bounded by smooth curved boundaries, using an alignment approach.

Alignment is a two-stage process. Given a model object and an image object, in the first stage a transformation is sought that would bring the model object to a position and orientation in space that corresponds to the projected image. Second, the appearance of the model following the transformation is predicted. The result is compared with the actual image, and the degree of match is used to decide whether the image is in fact an instance of the model.

The first stage of the alignment process, namely the search for an aligning transformation, will not be discussed here. The transformation may be determined by a small set of corresponding features, identified in both the model and the image. For example, three non-collinear points on the image and their corresponding points on the model determine uniquely the transformation [10, 17, 23, 12]. Two points and a line or three lines may also serve for this purpose [21].

1.1. The Prediction Problem

In this paper we address ourselves to the second stage of the alignment process. We present an approach for solving the following problem. Let $\mathcal{M} = \{M_1, M_2, \ldots, M_n\}$ be a set of object models. Let $\mathcal{T}$ be a set of transformations, that include rotations in 3D space, translations, and scale changes, followed by an orthographic projection. This projection model assumes that the object is not too close to the camera. Given a model $M \in \mathcal{M}$ and an aligning transformation $T \in \mathcal{T}$, predict the appearance of M in the image following the application of T.

The above definition of the set $\mathcal{T}$ of allowed transformation enables the prediction of the appearance of rigid objects from any given viewpoint. The general prediction problem extends the set $\mathcal{T}$ with other types of transformations, including, for example, articulated motion and distortion. This extension is beyond the scope of this paper.

In order to utilize edge maps in the image, we make the following definitions. Given an object O and a viewpoint v, the *rim* is the set of all the points on the object's surface, whose normal is perpendicular to the visual axis [14]. This set is also called the *contour generator* [18]. A *silhouette* is an image generated by the orthographic projection of the rim. In the analysis below we assume that every point along the silhouette is generated by a single rim point and that at the rim point the object lies to one

side of the line of sight (the line of sight does not "pierce" the object).

The prediction of the appearance of smooth objects is considerably more complex than the same prediction for objects with sharp edges. An edge map of an object usually contains the silhouette, which is generated by its rim. A rim that is generated by a sharp edge is stable on the object as long as the edge is visible. In contrast, a rim that is generated by a smooth surface changes continuously with the viewpoint.

The problem of predicting the new appearance of a smooth object following a rotation is illustrated in Fig. 1. The figure shows a bird's eye view of two rotating objects, a cube (a), (b) and an ellipsoid (c), (d). For both objects points p, q lie on the object's rim, and therefore their projections lie in the image on its silhouette. When the cube rotates from position (a) to (b), p, q remain on the rim. Their new 3D position is easily determined;
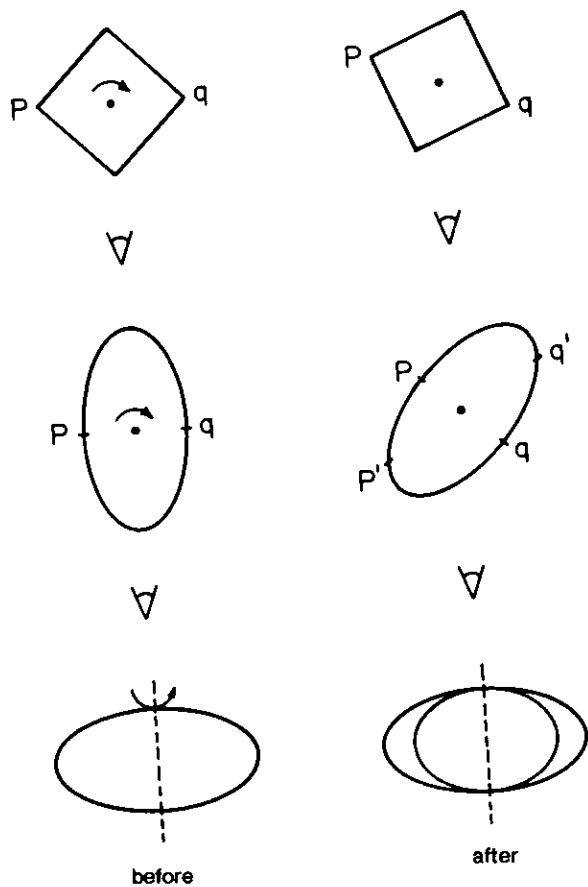

FIG. 1. Changes in the rim during rotation. (a) A bird's eye view of a cube. (b) The cube after rotation. In both (a) and (b) points p, q lie on the rim. (c) A bird's eye view of an ellipsoid. (d) The ellipsoid after rotation. The rim points p, q in (c) are replaced by p', q' in (d). (e) An ellipsoid in a frontal view. (f) The ellipsoid rotated (outer), superimposed on the appearance of the rim, as a space curve after rotation by the same amount (inner).

therefore the new silhouette can be predicted in a straightforward manner. In contrast, when the ellipsoid rotates from position (c) to (d), the new 3D position of p, q is no longer relevant since these points no longer lie on the object's rim. The silhouette is now generated by a new set of points p', q' in (d). Figures 1e, f show the ellipsoid in a frontal view before and after the rotation, compared to its appearance if the rim, as a space curve, had been rotated by the same amount. The conclusion is that the prediction problem for smooth objects is in general significantly more complicated than that of objects with sharp edges.

1.2. Previous Approaches

Most existing systems restrict themselves to polyhedral objects and ignore objects with smooth curved surfaces (e.g., [17, 12, 22]). Two approaches have been suggested in the past to solve this prediction problem for objects with smooth surfaces. The first approach describes an object as a composition of either volumetric or surface primitives that have simple geometrical structures [19, 4, 8, 20, 3, 9]. The transformation T is applied to each primitive. Since the primitives have simple geometrical structures, their silhouette can be predicted. The extreme points of the collection of the primitives' silhouettes are taken to be the object's silhouette. The second approach approximates the object's surface by a set of 3D wires [1]. The transformation T is applied to each wire. The extreme wires are taken to be the object silhouette.

The decomposition approach works well for simple objects, but usually not for complex ones. The wire approach is often costly from a computational standpoint due to the large number of wires required and the need to perform "hidden line elimination." Finally, these approaches usually enable the prediction of the bounding contours only. Internal contours and surface markings, that may have a significant role in shape-based recognition, are often not treated (e.g., [7]).

This paper presents an alternative approach for the prediction problem. In this approach an object is represented by its silhouette, as seen from a particular viewpoint. Using the 3D surface curvature of each point along the silhouette, it is possible to make an accurate estimation of the silhouette after the transformations. A few models of this kind are sufficient for predicting the object's appearance from any given viewpoint.

2. THE CURVATURE METHOD

The method is based on representing surface curvature of points along the silhouette. The basic idea is shown in Fig. 2. Let X and Y be the main axes of the image plane, and the Z-axis be the line of sight. Consider an object O
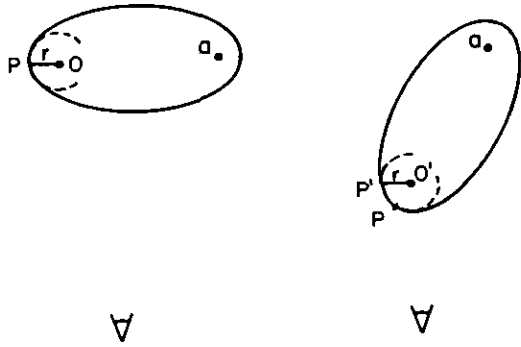
FIG. 2. The curvature method. (a) A horizontal section of an ellipsoid. p is a point on the rim, r is the radius of curvatures at p, o is the center of the curvature circle, and a is the intersection of the Y-axis with this section. (b) The section rotated. p' is the new rim point, and it is approximated by Eq. (1).

rotating by a rotation R about the vertical axis Y. Let p be a point on its rim. The figure shows a section of the object through p, that is perpendicular to Y. Let r_x be the curvature radius of p in this section, and let $\mathbf{r_x}$ be a vector of length r_x parallel to the X-axis. When the object rotates by R, point p ceases to be a rim point, and it is replaced by a new point p' approximated by

$$p' \approx R(p - \mathbf{r_x}) + \mathbf{r_x}. \qquad (1)$$

The meaning of Eq. (1) is the following. The point $o = p - \mathbf{r_x}$ is the center of the circle of curvature of p. To predict the new rim point we first apply R to o. Let $o' = R(p - \mathbf{r_x})$. The new rim point is then $p' = o' + \mathbf{r_x}$. This approximation holds as long as the circle of curvature provides a good approximation to the section at p.

It is worth noting that "sharp" boundaries, such as the cube edges in Fig. 1, or markings on the surface itself, do not require a special treatment. They are included in Eq. (1) as the special case $r_x = 0$.

So far we have considered rotations about the vertical Y axis. We shall next consider the effect on the silhouette of a rotation about an arbitrary axis in space. Any 3D rotation can be decomposed into two successive rotations: a rotation about some axis V in the image plane, followed by a second rotation about the Z-axis. The effect of rotating the object about the line of sight Z is, of course, easy to predict. The problem, therefore, is to predict the appearance of the object following a rotation about an axis V lying in the image plane.

In general, the vector of curvature radius $\mathbf{r_x}$ used in Eq. (1) would depend on the rotation axis. Let r_x, r_y be the radii of curvature at p for rotations about the Y and X axes, respectively. Proposition 1 below states that the radius of curvature for a rotation about any axis can be determined from r_x, r_y alone.

PROPOSITION 1. *Let p be a rim point, and let V_α be an axis lying within the image plane and forming an angle α with the X-axis. The curvature radius at p for rotations about V_α is given by*

$$r_\alpha = r_y \cos \alpha - r_x \sin \alpha. \qquad (2)$$

(A proof is given in Appendix A.)

From this proposition and Eq. (1) we can predict the position of p', the new rim point, for a rotation about an arbitrary axis within the image plane, and consequently any 3D axis as well, using the two parameters r_x, r_y at p. Proposition 2 below shows that, in fact, a single parameters suffices.

PROPOSITION 2. *Let $\mathbf{r} = (r_x, r_y)$ be the curvature vector at p, and let $\mathbf{t}$ be the tangent vector to the silhouette at p. Then $\mathbf{r} \cdot \mathbf{t} = 0$; that is, $\mathbf{r}$ is perpendicular to $\mathbf{t}$.*

(A proof is given in Appendix A.)

It follows from the two propositions above that a single number is sufficient to determine the radius of curvature for a rotation about any axis in the image plane. This number is the magnitude of the curvature vector, $\|\mathbf{r}\|$ (also called, the *radial curvature* at p [15, 3]). All other parameters can be derived from it as follows. Let θ be the angle between the tangent vector to the silhouette, $\mathbf{t}$, and the X-axis, then

$$\begin{aligned} r_x &= \|\mathbf{r}\| \sin \theta \\ r_y &= \|\mathbf{r}\| \cos \theta \qquad (3) \\ r_\alpha &= \|\mathbf{r}\| \cos(\theta + \alpha). \end{aligned}$$

Note that the curvature radii r_x, r_y, and r_α in general are not normal curvature radii of the surface, but rather oblique ones. They are generated from the intersection of the surface with planes that in general do not contain the surface normal. The radial curvature radius, $\|\mathbf{r}\|$, however, is a normal curvature radius (this follows directly from Proposition 2). Koenderink [15] and Brady *et al.* [3] proved that the gaussian curvature of the surface is the product of the radial curvature and the transverse curvature (the curvature of the projected contour at p). Giblin and Weiss [11] showed that additional curvature is required to compute the mean curvature of the surface. The curvature method requires neither the gaussian curvature, the mean curvature, nor the principal curvatures of the surface. Equation (3) above implies that the radial curvature is sufficient to recover the oblique curvature radii in all directions.

The scheme is therefore the following. An object model M is a 2D (orthographic) projection of its visible contours (including its sharp and smooth boundaries, as well as internal markings), as observed from a particular

viewing direction. To represent the entire object, a number of views would be required [13]. As shown in the examples below, this number is usually small. Each point along the silhouette has associated with it, along with its spatial coordinates, the radial curvature $\|\mathbf{r}\|$. Given a transformation T, translation, scaling, and rotation about the line of sight are applied to M in a straightforward manner. The effect of rotation about an arbitrary axis in the image plane is computed as follows. First, for each point on the model, the radius of curvature r with respect to the rotation axis is determined using Eq. (3). Once r is known, the new position of the point in the image is determined using Eq. (1), where instead of $\mathbf{r_x}$ a vector of size r perpendicular to the rotation axis is plugged in.

In this approach an object is represented using a number of viewer-centered descriptions, rather than a single object-centered representation. Each description covers a range of possible viewing angles, and to represent the entire object a number of descriptions are required. This number depends on the object shape and on the complexity of its aspect graph [13]. As shown in the examples below, this number is small for moderately complex objects. Using symmetries, the cars used in these examples required four models to cover all common views, which included all vertical rotations and elevation of $\pm30°$. Because of the orthographic projection approximation, if the object is to be recognized from both large distances as well as close-up views, additional models will be required. The computations required in this scheme during the prediction stage are simple; for example, no hidden-line elimination is necessary.

3. PROPERTIES OF THE CURVATURE METHOD

The appearance of objects with sharp boundaries (for which the radius of curvature is zero) and of spherical and cylinderal objects is predicted exactly by the curvature method. The appearance of smooth objects with arbitrary structures is, however, only approximated by this method. In order to demonstrate the properties of the curvature method, we applied this method to ellipsoids and analyzed the errors obtained. The analysis is given in this section. We first compute the errors obtained when a canonical ellipsoid rotates around the vertical (Y) axis. We then compute the errors obtained when the same ellipsoid rotates arbitrarily in 3D space and show that the errors obtained in the two cases are similar. The error depends on the shape of the ellipsoid, in other words, on the relative length of its axes, and it increases as the ellipsoid becomes "deep" (elongated in the Z-direction). We show that the errors are usually small, and that, in general, a small number of models is required to predict the appearance of an ellipsoid from all possible views.

We start with a brief explanation of the error function used. Consider an ellipsoid rotating about some axis V in

the image plane. Let $p_1 = (x_1, y_1)$ be the projected location of some rim point. Following rotation, the rim changes, and the point p_1 is replaced by a new point, $p_2 = (x_2, y_2)$, such that the vector $p_2 - p_1$ is perpendicular to V. Denote the approximated location of p_2 according to the curvature method by $\hat{p}_2 = (\hat{x}_2, \hat{y}_2)$. The observed error is measured by $\|\hat{p}_2 - p_2\|$. Clearly, if we scale the ellipsoid the observed error would scale as well. We therefore need instead to consider a relative value for the error that is independent of scale.

We define the error as follows. Consider the planar section through p_1 that is perpendicular to the rotation axis V. This section forms an ellipse (or a single point in case of a tangential section). Let $p_0 = (x_0, y_0)$ be the center of this ellipse. The relative error is defined by

$$E = \frac{\|\hat{p}_2 - p_2\|}{\|p_1 - p_0\|};$$

E reflects the observed error relative to the projected size of the ellipsoid. Note that E is independent of translation and scale of the ellipsoid.

3.1. Rotation around the Vertical Axis

Let

$$\frac{x^2}{a^2} + \frac{y^2}{b^2} + \frac{z^2}{c^2} = 1$$

be the surface of a canonical ellipsoid. Let $p_1 = (x_1, y_1)$ be a point on its silhouette. When the ellipsoid rotates about the vertical (Y) axis by an angle θ, p_1 disappears and is replaced by a new contour point $p_2 = (x_2, y_2)$ with an identical y-value, $y_2 = y_1$. Let $\hat{p}_2 = (\hat{x}_2, \hat{y}_2)$ be the approximated position of p_2 according to the curvature method. The horizontal section of the ellipsoid through p_1 is an ellipse centered around $p_0 = (0, y_0)$. Note that the points p_1, p_2, $\hat{p}_2$, and p_0 all lie on the same horizontal section, implying that $y_1 = y_2 = \hat{y}_2 = y_0$. The relative error is therefore reduced to

$$E = \left| \frac{\hat{x}_2 - x_2}{x_1} \right|.$$

(For reasons of convenience we ignore the absolute value operation in the discussion below.)

PROPOSITION 3. *The error is given by*

$$E\left(\frac{c^2}{a^2}, \theta\right) = \cos\theta + \frac{c^2}{a^2}(1 - \cos\theta)$$

$$- \sqrt{\cos^2\theta + (c^2/a^2)\sin^2\theta}.$$
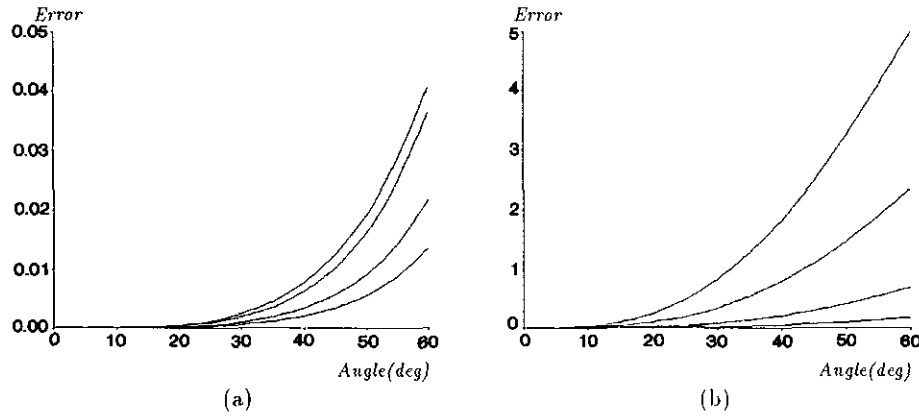
(4)

(A proof is given in Appendix B.)

FIG. 3. The errors of the curvature method as a function of θ, the angle of rotation. (a) $c^2/a^2 = \frac{1}{16}, \frac{1}{8}, \frac{1}{4}$, and $\frac{1}{2}$. (b) $c^2/a^2 = 2, 4, 9$, and 16. (The parameters correspond the curves at increasing heights.)

The expression obtained for the error depends on two parameters: the aspect ratio of the ellipsoid, c^2/a^2, and the angle of rotation, θ, and it is invariant under a uniform scaling of the ellipsoid.

3.2. Properties of the Error

The prediction error obtained by the curvature method for a canonical ellipsoid rotating about the Y-axis vanishes in the following three cases:

- $\theta = 0$ (that is, no rotation).
- $c^2/a^2 = 1$ (that is, $c = a$, the cross section is a circle).
- $c^2/a^2 = 0$ (that is, $c = 0$, a planar ellipsoid).

As a function of θ, the angle of rotation, the error function is symmetric; that is, similar errors are obtained both for positive and negative angles. The absolute value of the error increases monotonically with the absolute value of θ. The partial derivative E_θ also changes monotically with θ, so the error increases faster for larger values of θ. The derivative is given by

$$E_\theta = \left(1 - \frac{c^2}{a^2}\right) \sin \theta \left(\frac{\cos \theta}{\sqrt{\cos^2 \theta + (c^2/a^2) \sin^2 \theta}} - 1\right) \quad (5)$$

and assumes the following values:

- $E_\theta(0°) = 0$.
- $E_\theta(90°) = c^2/a^2 - 1$.

Figure 3 shows the error as a function of θ for several ellipses.

As a function of c^2/a^2, the relative size of the axes of the ellipsoid, the error behaves differently in each of the two ranges: (1) when $c \leq a$, and (2) when $c > a$. In the first case the ellipsoid's width is larger than its depth. The error assumes small values even for fairly large values of θ. The maximal error is obtained when

$$\frac{c^2}{a^2} = \frac{3}{4} - \frac{1}{2(1 + \cos \theta)} \quad (6)$$

and it assumes the following values:

- 0.24% at $30°$ $(c^2/a^2 = 0.482)$.
- 1.26% at $45°$ $(c^2/a^2 = 0.457)$.
- 4.14% at $60°$ $(c^2/a^2 = 0.417)$.

Figure 4 shows the maximal error as a function of θ.

When $c > a$, the ellipsoid is deeper than it is wide, the error assumes larger values and is unbounded when θ increases to $90°$. The partial derivative E_{c^2/a^2} increases monotonically with c^2/a^2 and reaches its maximum when $c^2/a^2 \to \infty$, where the error increases linearly in c^2/a^2. The derivative is given by

$$E_{c^2/a^2} = (1 - \cos \theta) - \frac{\sin^2 \theta}{\sqrt[2]{\cos^2 \theta + (c^2/a^2) \sin^2 \theta}} \quad (7)$$
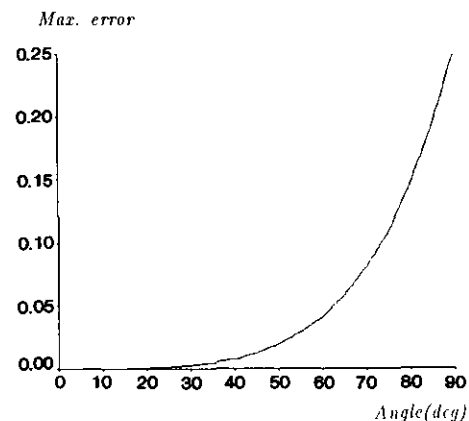

FIG. 4. The maximal value of the error for canonical ellipsoids with $c \leq a$ as a function of θ, the angle of rotation.
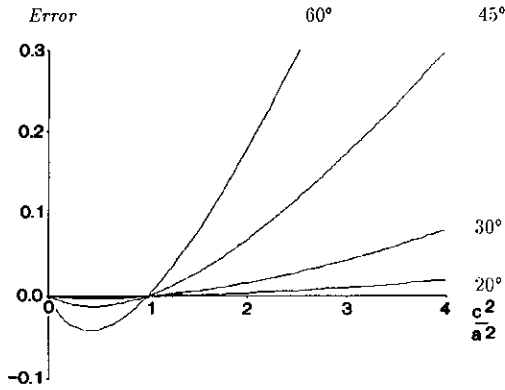
FIG. 5. The error as a function of the aspect ratio, c^2/a^2, of the ellipsoid for $\theta = 20°$, $30°$, $45°$, and $60°$. (The parameters correspond the curves at increasing magnitude.)

and assumes the following values:

- $E_{c^2/a_2}(0) = (1 - \cos \theta)^2/2 \cos \theta.$
- $E_{c^2/a_2}(1) = (1 - \cos \theta)^2/2.$
- $\lim_{c^2/a^2 \to \infty} E_{c^2/a_2} = 1 - \cos \theta.$

A model for such an ellipsoid would therefore cover only a restricted range of rotations. Larger rotations should be treated by additional models. Figure 5 shows the error as a function of c^2/a^2 for several values of θ.

When a complete set of models is prepared for the appearance of an ellipsoid to be predictable from all possible views, it should be considered that following a rotation of 90° about the Y-axis, a and c, the axes lengths of the ellipsoid, interchange their roles. Therefore, an ellipsoid with $c < a$ changes after a rotation of 90° to an ellipsoid with $c > a$. An ellipsoid with a high aspect ratio, c^2/a^2, changes to an ellipsoid with a low aspect ratio. Consequently, the small range of rotations covered by a model for an ellipsoid with a high aspect ratio is compensated by the large range of rotations covered by a model for the same ellipsoid after a 90° rotation. A small number of models is therefore required to represent the ellipsoid from all possible views.

Table 1 shows the number of models required to cover the entire range of rotations about the Y-axis for several ellipsoids. Because of symmetry considerations only rotations up to 90° should be considered. We see from the table that this number is small and does not exceed four, even for extreme aspect ratios and an allowed error of 1%.

In preparing this table each ellipsoid was initially represented by two models, one taken at its canonical position, the other following a 90° rotation. If the two models did not cover the entire range of rotations, additional models were added at intermediate positions. In this case

the value of the error is somewhat different than the canonical case. An expression describing this value is given in Appendix B.

3.3. Rotation in 3D Space

We now consider the case of a canonical ellipsoid rotating arbitrarily in 3D space. A rotation in 3D space can be decomposed into three successive rotations, about the X-, Y-, and Z-axes. The last rotation can be ignored since it does not deform the image and therefore does not change the errors. Let

$$\frac{(x \cos \alpha + y \sin \alpha)^2}{a^2} + \frac{(-x \sin \alpha + y \cos \alpha)^2}{b^2} + \frac{z^2}{c^2} = 1$$

be the surface of a canonical ellipsoid rotated about the Z-axis by an angle α. We now examine this ellipsoid as it rotates about the Y-axis by an angle θ.

PROPOSITION 4. The error is given by

$$E\left(\frac{C^2}{A^2}, \theta\right)$$

in Eq. (4), where

$$\frac{C^2}{A^2} = \frac{c^2}{a^2} \cos^2 \alpha + \frac{c^2}{b^2} \sin^2 \alpha. \tag{8}$$

(A proof is given in Appendix B.) Note that, depending on α, C^2/A^2 assumes any value between c^2/a^2 and c^2/b^2.

The consequence of Proposition 4 is that after an arbitrary rotation the appearance of an ellipsoid as it is approximated by the curvature method is in general neither better nor worse than its approximated appearance after a rotation about any of the main axes. As a result, if k models are required to cover all rotations around the X-axis, and k (or less) models cover all rotations around the Y-axis, then at most k^2 models are required to cover all possible rotations in 3D space.

TABLE 1
Number of Models as a Function of Allowed Error

$\dfrac{c^2}{a^2}$	1%	2%	3%	4%	5%	6%
2	3	3	2	2	2	2
4	3	3	3	3	2	2
9	4	3	3	3	3	2
16	4	3	3	3	3	2
49	4	3	3	3	2	2
100	4	3	3	2	2	2

4. MODEL CONSTRUCTION

We have implemented the alignment scheme described above and tested it on images of 3D objects. To apply the scheme, models of the viewed objects must be acquired. For our purpose, an object model must contain the spatial coordinates and the radii of curvature of the object's visible contours. The required 3D information can be obtained during a learning period using various 3D cues, such as stereo information and shading.

To estimate the radii of curvature we have used three edge pictures of each object. The radii of curvature are estimated using the following procedure. Consider three silhouette pictures (denoted by A, B, and C) that are taken from three different viewpoints along a circle in space perpendicular to the Y-axis (Fig. 6). Suppose α is the rotation angle between pictures A and B, and β is the rotation angle between pictures A and C. Let p_1, p_2, and p_3 be three corresponding points in A, B, and C, respectively. Since the camera was rotated about the Y-axis between successive pictures, all three points share the same y coordinate, so that $p_1 = (x_1, y, z_1)$, $p_2 = (x_2, y, z_2)$, and $p_3 = (x_3, y, z_3)$. According to Eq. (1)

$$x_2 = (x_1 - r_x) \cos \alpha + z_1 \sin \alpha + r_x \qquad (9)$$

$$x_3 = (x_1 - r_x) \cos \beta + z_1 \sin \beta + r_x. \qquad (10)$$

These are two linear equations of two unknown parameters z_1 and r_x. Hence

$$z_1 = \frac{x_1(\cos \alpha - \cos \beta) - x_2(1 - \cos \beta) + x_3(1 - \cos \alpha)}{(1 - \cos \alpha) \sin \beta - \sin \alpha(1 - \cos \beta)} \qquad (11)$$

$$r_x = \frac{x_1 \sin (\alpha - \beta) + X_2 \sin \beta - x_3 \sin \alpha}{(1 - \cos \alpha) \sin \beta - \sin \alpha(1 - \cos \beta)}. \qquad (12)$$

In the range $-\pi/2 < \alpha, \beta < \pi/2$, $\alpha \neq \beta$, the denominator does not vanish.

Equation (3) establishes that in general r_x and the tangent to the contour are sufficient to estimate the curva-
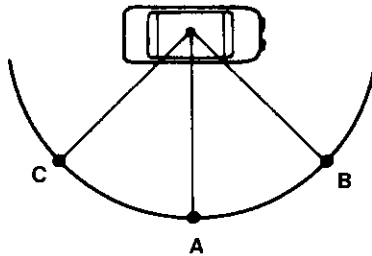

FIG. 6. Building a model using three edge pictures, a bird's eye view. Points A, B, and C are the three camera locations along a circle in space perpendicular to the Y-axis.

ture radius in all other directions. Nevertheless, this technique cannot be applied to points with a horizontal tangent. In this case $r_x = 0$, the curvature vector is horizontal, and its magnitude cannot be estimated from this set of images. To estimate the value of r_y at these points a similar procedure can be applied to three edge pictures obtained by a rotation about the X-axis. For contour points that their tangent is neither horizontal nor vertical this estimation of r_y is in principle redundant, but it can be used to improve the estimate of the curvature. In this manner five pictures can be used to create a model, three for a rotation about the X-axis, and three for a rotation about the Y-axis, with the central picture common to both sets. The final model consists of an edge map of the central picture, together with the depth coordinates and the estimated magnitude of the curvature vector (r_x, r_y) at each point.

Note that identifying corresponding points in the pictures is straightforward in this procedure. When the rotation is about the Y-axis, the corresponding points must lie on the same horizontal line. Each contour point therefore usually has a small number of candidate corresponding points to be considered. Details of this matching procedure will not be discussed here.

By setting $\beta = -\alpha$ the equations above can be simplified as

$$z_1 = \frac{x_2 - x_3}{2 \sin \alpha} \qquad (13)$$

$$r_x = \frac{x_2 + x_3 - 2x_1 \cos \alpha}{2(1 - \cos \alpha)}. \qquad (14)$$

If the angle α is not known, but assuming that α is small we can define new quantities $\hat{z}, \hat{r}_x$ as

$$\hat{z} = z\alpha \approx \frac{x_2 - x_3}{2} \qquad (15)$$

$$\hat{r}_x = (r_x - x_1)\alpha^2 \approx x_2 + x_3 - 2x_1. \qquad (16)$$

This approximation uses $\sin \alpha \to \alpha$ and $\cos \alpha \to 1 - \alpha^2/2$. In this case the aligning transformation should provide, instead of a rotation angle θ, the ratio θ/α,

$$x' \approx x + z\theta + (r_x - x) \frac{\theta^2}{2} = x + \hat{z}\left(\frac{\theta}{\alpha}\right) + \frac{\hat{r}_x}{2} \left(\frac{\theta}{\alpha}\right)^2. \qquad (17)$$

The ratio θ/α can be determined during the alignment process if we take these approximations into account. Suppose, for instance, that the alignment transformation is determined by a three-points correspondence. In this case a set of six equations describing rotation in 3D space, translation, and scale must be solved [23, 12]. If the three points lie on the object's contour, we can substi-

tute two of the six equations, those describing rotations about the X and Y axes, by Eq. (17). Consequently we obtain a new set of six equations with six unknown parameters to solve. This set will usually have a small number of solutions, but the details will not be considered further here. The range of rotations covered by a single model would depend on the object's shape and on the similarity to other models. The results shown in Section 5 also hold for this approximation.

The curvature method requires robust estimation of the curvature radii. The estimation of these radii from several images, however, was recently shown to be sensitive to camera calibration [25, 5]. We would like to make a few comments with respect to this point. First, the method presented in this section requires at least three images. Additional images can be used to improve the estimation. Other sources of structure information such as stereo and shading can also be used to achieve a robust estimation of the curvature radii.

Second, the curvature method, unlike the methods described in [25, 5] is relatively insensitive to calibration. The curvature radii in our method are used to predict the appearance of objects from different viewpoints. Instabilities in the computation are therefore significant only as long as they propagate into the predictions obtained. Equation (17) above implies that calibration errors, namely, errors in estimating the angle α, can be largely compensated in the prediction stage by changing the angle of rotation θ appropriately. As can be seen from Eq. (17), the prediction results depend on the ratio θ/α rather than on the exact value of α.

Finally, we tested the method described in this section for ellipsoids. Models of ellipsoids were constructed from
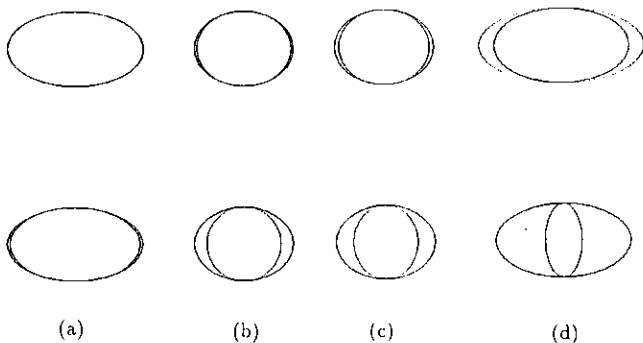

FIG. 7. Matching models of ellipsoids with their images. The curvature values in these models were estimated from three images of the ellipsoids obtained by rotating the ellipsoid about the vertical axis by angles $\pm\alpha$. The models were then rotated about the vertical axis by an angle θ, and the results were overlayed with the accurate image. Upper pictures: using the curvature method. Lower pictures: same experiments but the curvature is not used: (a) $c^2/a^2 = 0.5$, $\alpha = 60°$, $\theta = 30°$; (b) $c^2/a^2 = 0.5$, $\alpha = 30°$, $\theta = 60°$: (c) $c^2/a^2 = 2$, $\alpha = 60°$, $\theta = 30°$; (d) $c^2/a^2 = 2$, $\alpha = 30°$, $\theta = 60°$.

three images obtained by a rotation of $\pm60°$ and $\pm30°$ about the vertical axis. These models were then tested by rotating them by 30° and 60°, respectively, to obtain both interpolatory and extrapolatory predictions. The results are shown in Fig. 7. It can be seen that even when the curvature is estimated from only three images, the curvature method provides significantly better predictions of the appearance of the ellipsoids than when the curvature is not used.

5. IMPLEMENTATION

A prototype system for object recognition using alignment, that predicts the appearance of objects using the curvature method was implemented on a Symbolics 3670 Lisp machine. Pictures comprising of 512×512 pixels were taken, using a vidicon Cohu camera. Edge maps of the pictures were created using the Canny edge detector [6]. No smoothing operations were applied to the obtained edges. Toy models of two cars, a VW and a Saab, were assembled on a device that enables rotations about the vertical and the horizontal axes. Rotation angles can be controlled with this device up to moderate accuracy. The system first constructs object models comprising of depth values and curvature radii as described in Section 4. Models can be constructed in this system using either three images using rotations about the Y-axis, or five images using rotations about both the Y and X axes. The internal model can then be used to predict the appearance of the object following 3D rotation, translation, and scaling, using the curvature method described in Section 2. (An alternative implementation, using the linear combinations of 2D views, is described in [24].)

Two models of similar cars, a VW and a Saab, were created (Fig. 8). For each model three pictures were taken, with α and β (the angles between successive pictures, see Section 4) being $\pm30°$ about the Y-axis. For each car, the procedure resulted in a single model, comprising of the edge map of the central image, together with the approximated depth and curvature along the edges. It was found that a single model of this type yields accurate predictions to the appearance of the object within the entire 60° of rotation about the Y-axis.

Figure 9 shows four pictures, two of each car, rotated by $\pm15°$. Such rotations already create large deformations of the images (Fig. 10). Figure 11 shows the results of aligning the models with the images. An approximation to the transformation (rotation, translation, and scale) can be supplied by different alignment routines, e.g., using three corresponding points [23]. It can be seen that, by using the alignment procedure, a single model gives accurate fits to the object seen from different viewing positions. Figure 12 shows the result of matching the two cars with the incorrect models. The discrepancy between the image and the aligned model is significantly higher
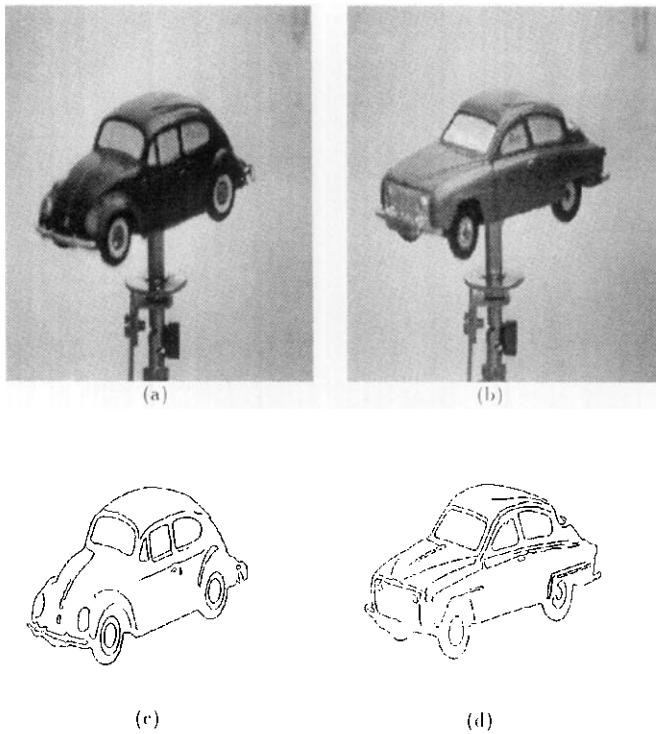
(a)

(b)

FIG. 8. The model objects: (a) a picture of the model VW car; (b) a picture of the model Saab car; (c) an edge map of the VW car; (d) an edge map of the Saab car.
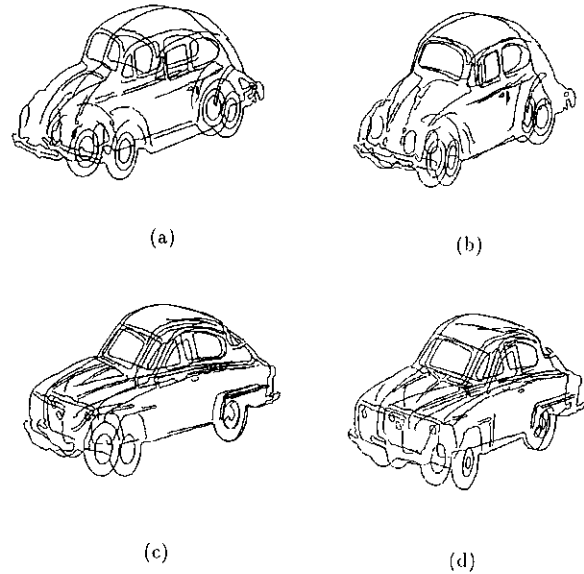

(a)

(b)

(c)

(d)

FIG. 10. Deformation of the images with respect to the models: (a) a deformation of the VW car following a rotation of −15°; (b) a deformation of the VW car following a rotation of +15°; (c) a deformation of the Saab car following a rotation of −15°; (d) a deformation of the Saab car following a rotation of +15°.

than in Fig. 11. A simple distance metric between the image contours and the aligned model was therefore sufficient to select the correct model. Figure 13 shows the

result of matching the two cars when the curvature information is not used. It can be seen that, while internal contours align perfectly, the occluding contours do not match as they do when the curvature is used. It is worth noting that accurate predictions were obtained despite the fact that (1) the objects have complex 3D shapes, and (2) we have used crude approximations to the radii of curvature using three pictures.

(a)

(b)

(c)

(d)

FIG. 9. The image objects: (a) a VW car rotated by −15° with respect to the model; (b) a VW car rotated by +15° with respect to the model; (c) a Saab car rotated by −15° with respect to the model; (d) a Saab car rotated by +15° with respect to the model.
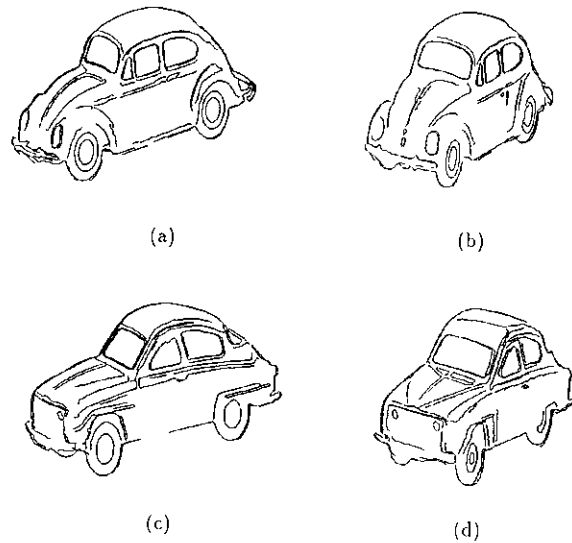

(a)

(b)

(c)

(d)

FIG. 11. Correct alignment of the models with the images: (a) alignment of the VW model with the first VW image; (b) alignment of the same VW model with the second VW image; (c) alignment of the Saab model with the first Saab image; (d) alignment of the same Saab model with the second Saab image.

(a)   (b)
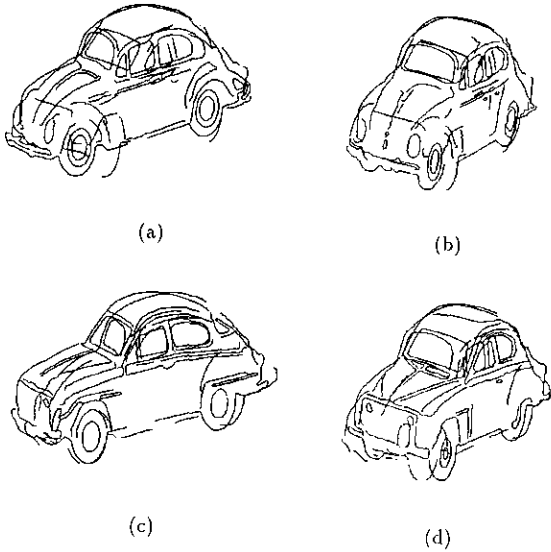
(c)   (d)

FIG. 12. Matching the images with incorrect models: (a) matching the first VW image to the Saab model; (b) matching the second VW image to the same Saab model; (c) matching the first Saab image to the VW model; (d) matching the second Saab image to the same VW model.

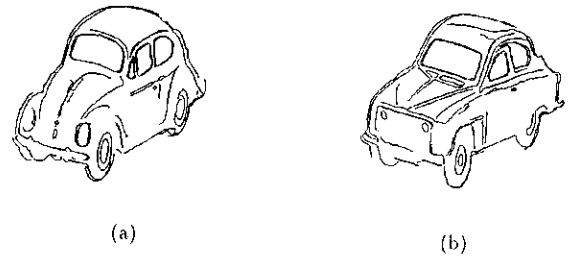(a)   (b)

FIG. 13. Matching the images with models that do not contain curvature information: (a) matching a VW image to a VW model; (b) matching a Saab image to a Saab model.

The curvature method described above is not restricted to contours originating from elliptic surface patches. It can as equally handle contours originating from hyperbolic patches—as long as the patches are visible. When, however, a patch is self-occluded, a new aspect of the object is observed, and an additional model should be utilized. The treatment of hyperbolic patches is demonstrated in Fig. 14. Models of three tori with different radii
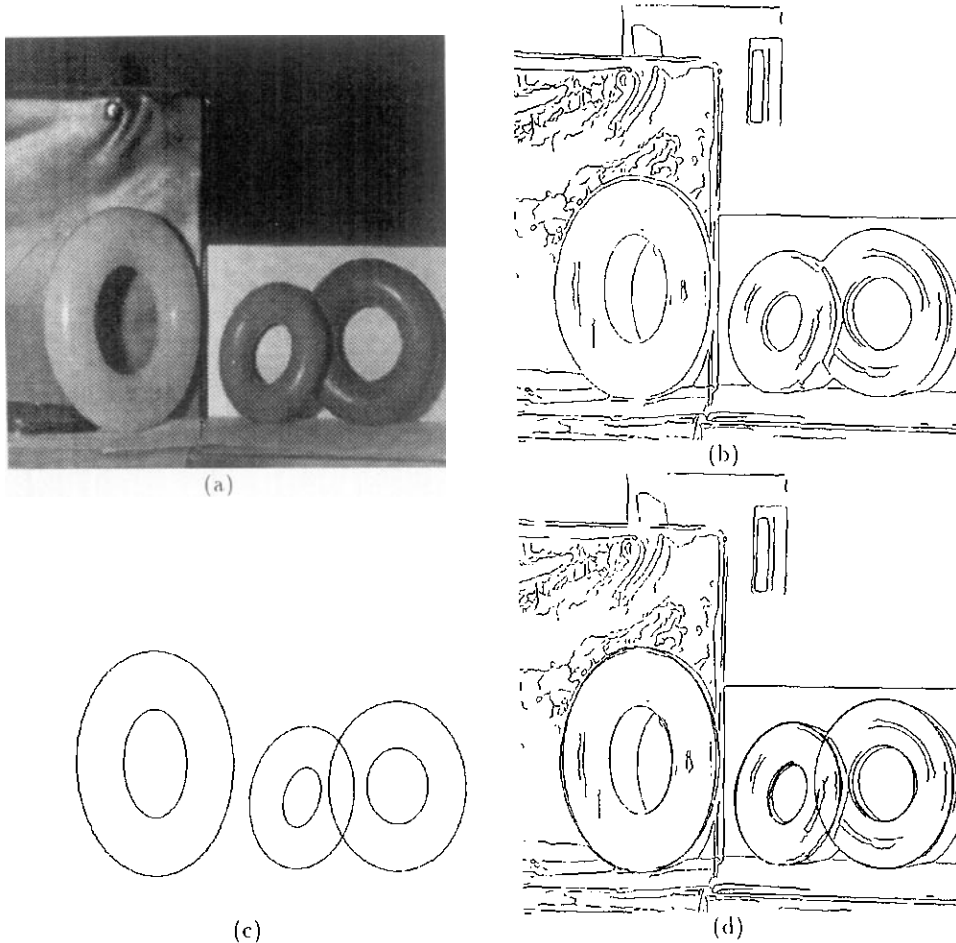

(a)

(b)

(c)

(d)

FIG. 14. (a) A picture of three tori. (b) A contour image of the tori. (c) A prediction of the appearance of the three tori. (d) Matching the prediction to the actual image.

were prepared analytically. The models were matched to an image that contained the tori in various positions and orientations. It can be seen that, although the points of the inner circles of the tori come from hyperbolic patches, their prediction is still accurate.

6. SUMMARY

In this paper we have proposed a method for predicting the new appearance of an object with a smooth surface, following a similarity transformation (3D rotation, translation, and scaling). The method uses the 3D surface curvature along the object contours. We have shown that a single parameter, the magnitude of the curvature vectors at these points, is sufficient to recover their curvature radii for a rotation about any given axis. Three pictures are in principle sufficient for approximating the radii of curvature for most contour points, and five can be used to estimate the components r_x, r_y independently.

The implemented scheme was found to give accurate results for large transformations. In the scheme we have proposed, each object is represented by a number of models, each covering a range of potential viewpoints. The results suggest that only a small number of such models are required to predict the new appearance of an object from any viewpoint.

APPENDIX A

Consider a surface defined by the implicit function $F(x, y, z) = 0$, F twice differentiable. Assuming an orthographic projection, where Z is the visual axis, the rim is defined by the set of points on the surface, where $F_z(x, y, z) = 0$. Let $p_0 = (x_0, y_0, z_0)$ be a rim point; that is, $F(p_0) = F_z(p_0) = 0$. We assume that either $F_x(p_0) \neq 0$ or $F_y(p_0) \neq 0$ and that $F_{zz}(p_0) \neq 0$. By this we ignore points with infinite radius of curvature and inflection points. These points may change their place unexpectedly during rotation.

LEMMA 1. *Let $F(x, y, z) = 0$ be a surface description, and let $p_0 = (x_0, y_0, z_0)$ be a rim point, i.e., $F(p_0) = F_z(p_0) = 0$. The curvature radii of p_0 with respect to the Y and X axes are given by*

$$r_x = -\frac{F_x}{F_{zz}}$$

$$r_y = -\frac{F_y}{F_{zz}}.$$

Proof. Consider the space curve defined by the implicit function $F(x, y_0, z) = 0$. According to the implicit function theorem, since $F_x(p_0) \neq 0$ and $F_{zz}(p_0) \neq 0$, $x(z)$ is a well-defined function in a neighborhood of p_0, and

$$\frac{d}{dz} F_z = F_{zz} + F_{zx}\left(\frac{dx}{dz}\right) = \frac{1}{F_x}(F_{zz}F_x - F_{zx}F_z)$$

$$\frac{d}{dz} F_x = F_{xz} + F_{xx}\left(\frac{dx}{dz}\right) = \frac{1}{F_x}(F_{xz}F_x - F_{xx}F_z).$$

And since

$$\frac{d^2x}{dz^2} = \frac{d}{dz}\left(\frac{dx}{dz}\right) = \frac{d}{dz}\left(-\frac{F_z}{F_x}\right)$$

$$= \frac{-\left(\frac{d}{dz}F_z\right)F_x + \left(\frac{d}{dz}F_x\right)F_z}{F_x^2},$$

we obtain

$$\frac{d^2x}{dz^2} = \frac{-F_{zz}F_x^2 + F_{zx}F_xF_z + F_{xz}F_xF_z - F_{xx}F_z^2}{F_x^3}.$$

$F_z(p_0) = 0$, therefore

$$\frac{dx}{dz}(z_0) = 0$$

$$\frac{d^2x}{dz^2}(z_0) = -\frac{F_{zz}}{F_x}.$$

For a curve $x(z)$, the radius of curvature at z_0 is given by

$$r(t) = \frac{1}{k(t)} = \frac{(1 + (dx/dz)(z_0))^{3/2}}{(d^2x/dz^2)(z_0)}.$$

Substituting the appropriate terms we obtain

$$r_x = -\frac{F_x}{F_{zz}}$$

and, in a similar way,

$$r_y = -\frac{F_y}{F_{zz}}.$$

PROPOSITION 1. *Let $F(x, y, z) = 0$ be a surface description, and let p_0 be a rim point; i.e., $F(p_0) = F_z(p_0) = 0$. Let V_α be an axis lying in the image plane and forming an angle α with the positive X-axis. The radius of curvature at p_0 with respect to V_α is given by*

$$r_\alpha = r_y \cos \alpha - r_x \sin \alpha.$$

Proof. Let $G(x', y', z) = 0$ be the surface $F(x, y, z) = 0$ rotated about the Z-axis by the angle $-\alpha$; i.e.,

$$G(x', y', z) = F(x' \cos \alpha - y' \sin \alpha, x' \sin \alpha + y' \cos \alpha, z).$$

After such a rotation V_α coincides with the X-axis; therefore

$$r_\alpha^F = r_{y'}^G$$

Where r^F, r^G are radii of curvature for the surfaces F, G, respectively. According to Lemma 1,

$$r_{y'}^G = -\frac{G_{y'}}{G_{zz}}.$$

Since

$$G_{y'} = -F_x \sin\alpha + F_y \cos\alpha$$

$$G_z = F_z = 0$$

$$G_{zz} = F_{zz}$$

we obtain

$$r_\alpha = \frac{-F_y \cos\alpha + F_x \sin\alpha}{F_{zz}} = r_y \cos\alpha - r_x \sin\alpha.$$

PROPOSITION 2. *Let* $F(x, y, z) = 0$ *be a surface description, and let* p_0 *be a rim point; i.e.,* $F(p_0) = F_z(p_0) = 0$. *Let* $\mathbf{r} = (r_x, r_y)$ *be the curvature vector at* p_0, *and let* $\mathbf{t}$ *be the tangent vector to the silhouette at* p_0. *Then* $\mathbf{r} \cdot \mathbf{t} = 0$; *that is,* $\mathbf{r} \perp \mathbf{t}$.

Proof. The point p_0 satisfies the two constraints $F(p_0) = 0$ and $F_z(p_0) = 0$. According to the implicit function theorem, since $F_y(p_0) \neq 0$, $F_{zz}(p_0) \neq 0$, $y(x)$, $z(x)$ are well-defined functions in a neighborhood of p_0. The tangent vector $\mathbf{t}$ to $y(x)$ is in the direction $(1, dy/dx)$ in the XY plane, and since $dy/dx = -F_x/F_y$, $\mathbf{t}$ is the direction $(-F_y, F_x)$. According to Lemma 1, the vector of curvature radii is given by

$$\mathbf{r} = (r_x, r_y) = \left(-\frac{F_x}{F_{zz}}, -\frac{F_y}{F_{zz}}\right).$$

Therefore

$$\mathbf{r} \cdot \mathbf{t} = \frac{F_x F_y}{F_{zz}} - \frac{F_x F_y}{F_{zz}} = 0.$$

APPENDIX B

In this appendix we derive an expression of the error obtained when the curvature method is applied to a canonical ellipsoid rotating about the vertical axis. We then show that a similar error is obtained when the ellipsoid is rotating about any axis in space. Finally, we compute the

error resulting from applying the curvature method to a non-canonical ellipsoid.

B.1. *Rotation about the Vertical Axis*

Let

$$\frac{x^2}{a^2} + \frac{y^2}{b^2} + \frac{z^2}{c^2} = 1$$

be the surface of a canonical ellipsoid. Let $p_1 = (x_1, y_1)$ be a point on its silhouette. Assume the ellipsoid is rotating about the vertical (Y) axis by an angle θ. Let $p_2 = (x_2, y_2)$ be the apparent position of p_1 following the rotation, and let $\hat{p}_2 = (\hat{x}_2, \hat{y}_2)$ be the approximate position of p_2 according to the curvature method. The relative error for the case of an ellipsoid that is rotating about the Y-axis is given by

$$E = \frac{\hat{x}_2 - x_2}{x_1}.$$

PROPOSITION 3. *The error is given by*

$$E\left(\frac{c^2}{a^2}, \theta\right) = \cos\theta + \frac{c^2}{a^2}\left(1 - \cos\theta\right)$$
$$- \sqrt{\cos^2\theta + (c^2/a^2)\sin^2\theta}.$$

Proof. The rim of a canonical ellipsoid contains the surface points for which $z = 0$. Therefore, the silhouette is defined by

$$\frac{x^2}{a^2} + \frac{y^2}{b^2} = 1.$$

After the ellipsoid is rotated by an angle θ about the Y-axis, it is described by

$$\frac{(x\cos\theta - z\sin\theta)^2}{a^2} + \frac{y^2}{b^2} + \frac{(x\sin\theta + z\cos\theta)^2}{c^2} = 1.$$

And its silhouette is given by

$$\frac{x^2}{a^2\cos^2\theta + c^2\sin^2\theta} + \frac{y^2}{b^2} = 1.$$

The position of $p_2 = (x_2, y_2)$ is therefore

$$x_2 = \frac{x_1}{a}\sqrt{a^2\cos^2\theta + c^2\sin^2\theta}$$

$$y_2 = y_1.$$

Next we calculate $\hat{p}_2$. Denote the surface of the canonical ellipsoid by the form $F(x, y, z) = 1$. According to

Lemma 1 (Appendix A) the curvature radius with respect to the Y-axis is given by

$$r_x = -\frac{F_x}{F_{zz}} = -\frac{c^2 x}{a^2}.$$

When the ellipsoid rotates about the Y-axis by an angle θ, the position of p_2 is estimated by the curvature method to be

$$\hat{x}_2 = x_1 \cos \theta - \frac{c^2 x_1}{a^2}(1 - \cos \theta)$$

$$\hat{y}_2 = y_1.$$

Consequently, the relative error is given by

$$E\left(\frac{c^2}{a^2}, \theta\right) = \frac{\hat{x}_2 - x_2}{x_1} = \cos \theta + \frac{c^2}{a^2}(1 - \cos \theta)$$
$$- \sqrt{\cos^2 \theta + (c^2/a^2) \sin^2 \theta}.$$

The error is therefore a function of θ and c^2/a^2.

B.2. *Rotation in 3D Space*

In this section we consider the case of a canonical ellipsoid rotating arbitrarily in 3D space. A rotation in 3D space can be decomposed into three successive rotations, about the Z-, Y-, and Z-axes. The last rotation can be ignored since it does not deform the image and therefore does not change the errors. (The first rotation cannot be ignored since it determines the actual axis of the second rotation.) Let

$$\frac{(x \cos \alpha + y \sin \alpha)^2}{a^2} + \frac{(-x \sin \alpha + y \cos \alpha)^2}{b^2} + \frac{z^2}{c^2} = 1$$

be the surface of a canonical ellipsoid rotated about the Z-axis by an angle α. We now examine this ellipsoid as it rotates about the Y-axis by an angle θ.

PROPOSITION 4. *The error is given by*

$$E\left(\frac{C^2}{A^2}, \theta\right),$$

where

$$\frac{C^2}{A^2} = \frac{c^2}{a^2}\cos^2 \alpha + \frac{c^2}{b^2}\sin^2 \alpha.$$

Proof. In order to prove this proposition we have to show that every horizontal section of the ellipsoid defined above is an ellipse with an aspect ratio C^2/A^2 as given in the proposition.

Any nonempty intersection of an ellipsoid and a plane is either a point or an ellipse. The section is nonempty when $y^2 \le a^2 \sin^2 \alpha + b^2 \cos^2 \alpha$, and is a point when a strict equality holds. Given the canonical ellipsoid following its rotation about the Z-axis by an angle α, we show that the boundaries of its horizontal section can be represented as

$$\frac{(x - x_0)^2}{A^2} + \frac{z^2}{C^2} = 1$$

which describes a canonical ellipse displaced along the X-axis. To establish the above relation, we show that for a constant value of y the surface equation of the rotated ellipsoid reduces to the equation of the displaced ellipse. The two equations are identical if there exists a constant $k \ne 0$ such that the following equation system holds

$$kC^2 = \frac{\cos^2 \alpha}{a^2} + \frac{\sin^2 \alpha}{b^2}$$

$$kC^2 x_0 = y \sin \alpha \cos \alpha \left(\frac{1}{b^2} - \frac{1}{a^2}\right)$$

$$kA^2 = 1/c^2$$

$$kC^2(A^2 - x_0^2) = 1 - y^2 \left(\frac{\sin^2 \alpha}{a^2} + \frac{\cos^2 \alpha}{b^2}\right).$$

We obtain a system of four equations in four unknowns, A^2, C^2, x_0, and k. We now show that when $y^2 < a^2 \sin^2 \alpha + b^2 \cos^2 \alpha$ this system has a unique solution with positive values for A^2 and C^2.

Denote the right side of the four equations by

$$p = \frac{\cos^2 \alpha}{a^2} + \frac{\sin^2 \alpha}{b^2}$$

$$q = y \sin \alpha \cos \alpha \left(\frac{1}{b^2} - \frac{1}{a^2}\right)$$

$$r = 1/c^2$$

$$s = 1 - y^2 \left(\frac{\sin^2 \alpha}{a^2} + \frac{\cos^2 \alpha}{b^2}\right).$$

The solution to the system above is given by

$$x_0 = \frac{kC^2 x_0}{kC^2} = \frac{q}{s}$$

$$A^2 = \frac{kC^2(A^2 - x_0^2) + kC^2 x_0^2}{kC^2} = \frac{ps + q^2}{p^2}$$

$$C^2 = \frac{kC^2(A^2 - x_0^2) + kC^2 x_0^2}{kA^2} = \frac{ps + q^2}{pr}$$

$$k = \frac{kA^2}{A^2} = \frac{p^2 r}{ps + q^2}.$$

Note that $p, r > 0$. This system therefore has a unique solution with positive values for A^2 and C^2 when $ps + q^2 > 0$. This inequality is satisfied when $y^2 < a^2 \sin^2 \alpha + b^2 \cos^2 \alpha$.

Now, we can compute the value of the ratio C^2/A^2 from this equation system by dividing the first equation by the third one:

$$\frac{C^2}{A^2} = \frac{c^2}{a^2} \cos^2 \alpha + \frac{c^2}{b^2} \sin^2 \alpha.$$

Therefore, any horizontal section of this ellipsoid is an ellipse with an aspect ratio of C^2/A^2, and since translation does not affect the results of the curvature method, the error is given by

$$E\left(\frac{C^2}{A^2}, \theta\right),$$

where A^2 and C^2 are the parameters of the ellipse and θ is the rotation angle about the Y-axis.

B.3. Intermediate Models

In this section we derive an expression of the error obtained when the curvature method is applied to an ellipsoid that is rotated about the Y-axis (rather than a canonical ellipsoid). This computation is required for constructing Table 1 in Section 3.2. Let

$$\frac{(x \cos \alpha - z \sin \alpha)^2}{a^2} + \frac{y^2}{b^2} + \frac{(x \sin \alpha + z \cos \alpha)^2}{c^2} = 1$$

be the surface of a canonical ellipsoid rotated about the Y-axis by an angle α. Assume this ellipsoid is modeled by the curvature method. We consider now the error produced by using this model as the ellipsoid rotates about the Y-axis by an angle θ.

PROPOSITION 5. *The relative error is given by*

$$E_\alpha\left(\frac{c^2}{a^2}, \theta\right) = \cos \theta + z' \sin \theta + r'(1 - \cos \theta) - x'',$$

where

$$z' = -\frac{\sin \alpha \cos \alpha (1 - c^2/a^2)}{\cos^2 \alpha + (c^2/a^2) \sin^2 \alpha}$$

$$r' = \frac{c^2/a^2}{(\cos^2 \alpha + (c^2/a^2) \sin^2 \alpha)^2}$$

$$x'' = \sqrt{\frac{\cos^2(\alpha + \theta) + (c^2/a^2) \sin^2(\alpha + \theta)}{\cos^2 \alpha + (c^2/a^2) \sin^2 \alpha}}.$$

Proof. Let $p_1 = (x_1, y_1)$ be a point on the silhouette of the ellipsoid. Let z_1 be its depth value, and let r_1 be its curvature value with respect to the Y-axis. Then

$$x_1 = (x/a) \sqrt{a^2 \cos^2 \alpha + c^2 \sin^2 \alpha}$$

$$y_1 = y$$

$$z_1 = \frac{-x \sin \alpha \cos \alpha (a^2 - c^2)}{a \sqrt{a^2 \cos^2 \alpha + c^2 \sin^2 \alpha}}$$

$$r_1 = \frac{xac^2}{(a^2 \cos^2 \alpha + c^2 \sin^2 \alpha)^{3/2}},$$

where $p = (x, y)$ is the corresponding point on the silhouette of the ellipsoid in its canonical position.

Let $p_2 = (x_2, y_2)$ be the apparent position of p_1 after a rotation about the Y-axis by an angle θ, p_2 is given by

$$x_2 = (x/a) \sqrt{a^2 \cos^2(\alpha + \theta) + c^2 \sin^2(\alpha + \theta)}$$

$$y_2 = y.$$

Let $\hat{p}_2 = (\hat{x}_2, \hat{y}_2)$ be the position of p_2 approximated by the curvature method

$$\hat{x}_2 = x_1 \cos \theta + z_1 \sin \theta + r_1(1 - \cos \theta)$$

$$\hat{y}_2 = y.$$

Since $y_1 = y_2 = \hat{y}_2$, the error is defined by

$$E_\alpha = \frac{\hat{x}_2 - x_2}{x_1}.$$

Let

$$z' = z_1/x_1$$

$$r' = r_1/x_1$$

$$x'' = x_2/x_1$$

and we obtain the expressions given in the proposition. Note that

$$E_0\left(\frac{c^2}{a^2}, \theta\right) = E\left(\frac{c^2}{a^2}, \theta\right)$$

in Eq. (4).

ACKNOWLEDGMENTS

REFERENCES

1. H. Baker, Three-dimensional modeling, in *Proceedings, 5th Int. Joint Conf. on Artificial Intelligence, Cambridge, MA, Aug. 22–25, 1977, IJCAI*, pp. 649–655.

2. R. Basri and S. Ullman, The alignment of objects with smooth surfaces, in *Proceedings, 2nd Int. Conf. of Computer Vision, Florida, 1988*, pp. 482–488.

3. M. Brady, J. Ponce, A. Yuille, and H. Asada, Describing surfaces, *A.I. Memo 882*, in *Artificial Intelligence*, Vol. 17, pp. 285–349, Vieweg, Brunswick, 1985.

4. C. M. Brown, Some mathematical and representational aspects of solid modeling, *IEEE Trans. Pattern Anal. Mach. Intell.* **3**, No. 4, 1981.

5. A. Blake and R. Cipolla, in *Proceedings, 1st European Conf. of Computer Vision, Antibes, France, 1990*, pp. 465–474.

6. J. Canny, *Finding Edges and Lines in Images*, MIT Artificial Intelligence Laboratory Report AI-TR-720, 1983.

7. C. H. Chien and J. K. Aggarwal, Shape recognition from single silhouette, in *Proceedings, ICCV Conf., London, 1987*, pp. 481–490.

8. C. Dane and R. Bajcsy, An object-centered three-dimensional model builder, in *Proceedings, 6th Int. Conf. Pat. Recog., Munich, Germany, Oct. 19–22, 1982*, pp. 348–350.

9. O. D. Faugeras and M. Hebert, The representation, recognition and location of 3-D objects, *Int. J. Rob. Res.* **5**(3), 1986, 27–52.

10. M. A. Fischler and R. C. Bolles, Random sample consensus: A paradigm for model fitting with application to image analysis and automated cartography, *Commun. ACM* **24**(6), 1981, 381–395.

11. P. Giblin and R. Weiss, Reconstruction of surfaces from profiles, in *Proceedings, ICCV Conf., London, 1987*, pp. 136–144.

12. D. P. Huttenlocher and S. Ullman, Object recognition using alignment, in *Proceedings, ICCV Conf., London, 1987*, pp. 102–111.

13. J. J. Koenderink and A. J. Van Doorn, The internal representation of solid shape with respect to vision, *Biol. Cybernet.* **32**, 1979, 211–216.

14. J. J. Koenderink and A. J. Van Doorn, The shape of smooth objects and the way contours end, *Perception* **11**, 1981, 129–137.

15. J. J. Koenderink, What does the occluding contour tell us about solid shapes?, *Perception* **13**, 1984, 321–330.

16. Y. Lamdan, J. T. Schwartz, and H. Wolfson, *On Recognition of 3-D Objects from 2-D Images*, Courant Institute of Mathematical Sciences, Robotics Technical Report 122, 1987.

17. D. G. Lowe, *Three-dimensional object recognition from single two-dimensional images*, Robotics Research Technical Report 202, Courant Institute of Math. Sciences, New York University, 1985.

18. D. Marr, Analysis of occluding contour, *Philos. Trans. R. Soc. London B* **275**, 1977, 483–524.

19. D. Marr and H. K. Nishihara, Representation and recognition of the spatial organization of three dimensional shapes, *Proc. R. Soc. B* **200**, 1978, 269–291.

20. M. Potmesil, 1983. Generating models of solid objects by matching 3-D surface segments, in *Proceedings, 8th Int. Joint Conf. Art. Intell., Karlsruhe, Germany, Aug. 8–12, 1983*, pp. 1089–1093.

21. D. Shoham and U. Ullman, Aligning a model to an image using minimal information, in *Proceedings 2nd ICCV Conference, Florida, 1988*, pp. 259–263.

22. D. W. Thompson and J. L. Mundy, 1987. Three-dimensional model matching from an unconstrained viewpoint, in *Proceedings, IEEE Int. Conf. on Robotics and Automation, Raleigh, NC, 1987*, pp. 208–220.

23. S. Ullman, Aligning pictorial descriptions: An approach to object recognition, *Cognition* **32**, No. 3, 1989, 193–254; A.I. Memo 931, The Artificial Intelligence Lab., MIT, 1986.

24. S. Ullman and R. Basri, Recognition by linear combinations of models, *IEEE Trans. Pattern Anal. Mach. Intell.* **13**, No. 10, 1991, 992–1006.

25. R. Vaillant and O. D. Faugeras, Using occluding contours for recovering shape properties of objects, *IEEE Workshop on Interpretation of 3D Scenes, 1989*, pp. 26–32.